

# Organic & Biomolecular Chemistry

Accepted Manuscript



This article can be cited before page numbers have been issued, to do this please use: J. A. Izzo, Y. Myshchuk, J. S. Hirschi and M. J. Vetticatt, *Org. Biomol. Chem.*, 2019, DOI: 10.1039/C9OB00072K.



This is an Accepted Manuscript, which has been through the Royal Society of Chemistry peer review process and has been accepted for publication.

Accepted Manuscripts are published online shortly after acceptance, before technical editing, formatting and proof reading. Using this free service, authors can make their results available to the community, in citable form, before we publish the edited article. We will replace this Accepted Manuscript with the edited and formatted Advance Article as soon as it is available.

You can find more information about Accepted Manuscripts in the [author guidelines](#).

Please note that technical editing may introduce minor changes to the text and/or graphics, which may alter content. The journal's standard [Terms & Conditions](#) and the ethical guidelines, outlined in our [author and reviewer resource centre](#), still apply. In no event shall the Royal Society of Chemistry be held responsible for any errors or omissions in this Accepted Manuscript or any consequences arising from the use of any information it contains.

## Transition State Analysis of an Enantioselective Michael Addition by a Bifunctional Thiourea Organocatalyst

 Joseph A. Izzo, Yaroslav Myshchuk,<sup>†</sup> Jennifer S. Hirschi,<sup>\*</sup> and Mathew J. Veticcatt<sup>\*</sup>

 WonReceived 00th January 20xx,  
Accepted 00th January 20xx

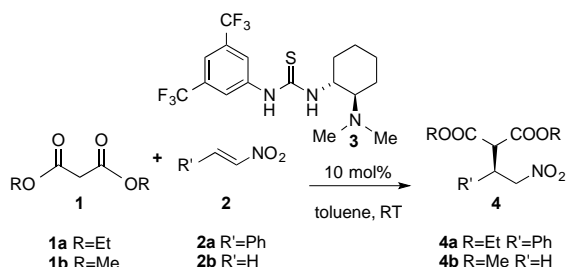
DOI: 10.1039/x0xx00000x

www.rsc.org/

The mechanism of the enantioselective Michael Addition of diethyl malonate to *trans*- $\beta$ -nitrostyrene catalyzed by a tertiary amine thiourea organocatalyst is explored using experimental <sup>13</sup>C kinetic isotope effects and density functional theory calculations. Large primary <sup>13</sup>C KIEs on the bond-forming carbon atoms of both reactants suggest that carbon-carbon bond formation is the rate-determining step in the catalytic cycle. This work resolves conflicting mechanistic pictures that have emerged from prior experimental and computational studies.

### Introduction

In 2003, Takemoto and co-workers introduced chiral bifunctional thioureas as a powerful class of organocatalysts for the enantioselective addition of malonates (**1**) to nitro olefins (**2**).<sup>1</sup> Since this initial report, the tertiary amine thiourea catalyst **3** has been used in a diverse array of enantioselective transformations including the aza-Henry reaction,<sup>2</sup> dynamic kinetic resolution of aza-lactones,<sup>3</sup> Michael addition to  $\alpha,\beta$ -unsaturated imides,<sup>4</sup> the aldol reaction,<sup>5</sup> *sp*<sup>2</sup>-alkylations,<sup>6</sup> and spiro-ketal formation<sup>7</sup> as some important examples. Additionally, success of the Takemoto catalyst (**3**) has inspired the design and development of several new chiral scaffolds involving variation of the groups that flank the thiourea

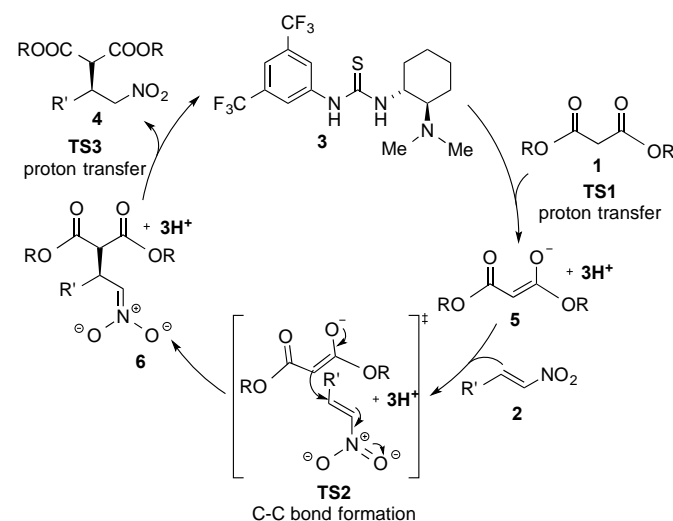


**Scheme 1.** Enantioselective Michael addition of nitro olefins to malonates catalyzed by bifunctional thiourea **3**.

 moiety.<sup>8</sup>

Over the past decade, the dual substrate mode of activation – simultaneous activation of both reacting partners – has emerged as one of the mainstays of asymmetric organocatalysis.<sup>9</sup> The proposed mechanism for the Michael addition of **1** to **2** begins with initial deprotonation of **1** (**TS1**) by

the tertiary amine moiety of **3** resulting in protonated catalyst-enolate complex **5**. The protonated chiral catalyst **3H**<sup>+</sup> directs the addition of enolate to the *si*-face of **2** (**TS2**) resulting in protonated catalyst nitronate complex **6**. Proton transfer from **3H**<sup>+</sup> to the nitronate (**TS3**) yields product **4** and regenerates the catalyst **3**. Kinetic studies by Takemoto and co-workers show that the reaction is first order in **1a**, **2a** and **3** – strongly supporting **TS2** as the rate-determining step in the catalytic



**Scheme 2.** Catalytic cycle for bifunctional thiourea catalyzed Michael Addition cycle.<sup>10</sup>

Takemoto's experimental studies were followed by two conflicting computational studies investigating the origin of enantioselectivity and identity of the rate-determining step.<sup>11</sup> A theoretical study by Liu and co-workers, utilized DFT calculations on the Michael addition of dimethylmalonate (**1b**) to 1-nitropropene (**2b**) using a truncated model of **3** (the aromatic moiety replaced by a hydrogen atom) as the model system to compute the energetics of the reaction coordinate.<sup>11a</sup> This study concludes that proton transfer from **3H**<sup>+</sup> to the nitronate carbon (**TS3**) is the rate-determining step in the catalytic cycle. Even though competing protonation of the nitronate oxygen was calculated as a lower energy pathway, the authors claim that the barrier for the tautomerization step (the

<sup>a</sup> Department of Chemistry, Binghamton University, Binghamton, NY 13902, USA

<sup>\*</sup>veticcatt@binghamton.edu

<sup>\*</sup>jhirschi@binghamton.edu

<sup>†</sup> Current address: Department of Chemistry, University at Buffalo, The State University of New York, Buffalo, NY 14260.

Electronic Supplementary Information (ESI) available: [details of any supplementary information available should be included here]. See DOI: 10.1039/x0xx00000x

product resulting from proton transfer from O to C in the product nitronate) is too high in energy to make this pathway accessible. Pápai and co-workers investigated the organization of the carbon-carbon bond-forming **TS2** using **1b** and **2a** as model reactants and unmodified catalyst **3**.<sup>11b</sup> This study identified two viable binding modes for **TS2** (Fig 1). In binding mode A, **2a** is H-bonded to the thiourea moiety and the enolate of **1b** is H-bonded to the protonated tertiary amine; conversely, binding mode B corresponds to structures with the enolate of **1b** is H-bonded to the thiourea moiety and **2a** is H-bonded to the protonated tertiary amine. Pápai calculated binding mode B as energetically favored by 2.7 kcal/mol (E+zpe). The TS for initial deprotonation of **1a** (TS1) was calculated as lower in energy by 2.9 kcal/mol than the lowest energy transition state structure located for TS2. Based on these observations, Pápai proposed that carbon-carbon bond formation is the rate-determining step.

Since the initial proposal of the two classic binding modes A and B by Pápai, transition state models with subtle variations have been explored by several theoretical studies.<sup>12</sup> For example, a binding mode was proposed by Zhong and co-workers for the

Michael addition to diketoenes (Zhong model Fig 1).<sup>13</sup> This mode is similar to binding mode B but with an additional hydrogen bond to the achiral aryl group. This binding mode has been proposed in 1,3-dipolar cycloadditions as well.<sup>14</sup> In another example, two additional binding modes were proposed by Wong and co-workers for a related squaramide system (Wong and Wong').<sup>15</sup> In addition, several NMR, crystallographic, and computational studies on similar systems have proposed that the lowest energy binding conformation of the catalyst adopts a "syn,anti" configuration of the thiourea functional group and not the traditional thiourea "anti,anti" configuration. An example of catalysis by this unique binding mode was proposed by Schreiner for the binding of benzoic acid to the thiourea catalyst (Fig 1).<sup>16</sup>

Considering the broad interest in the title reaction (700+ citations for Takemoto's original report) and the widespread use of tertiary amine thioureas as asymmetric organocatalysts, we decided to study the Michael addition of **1a** to **2a** catalyzed by thiourea **3** using experimental kinetic isotope effects (KIEs) and theoretical studies. Experimental KIEs probe the rate-determining step of a reaction, and in conjunction with theory, provide valuable insight into the transition state geometry of this isotope sensitive step. We report herein the results of our study which confirms rate-determining C-C bond formation (**TS2**) as the mechanism of this transformation. Comprehensive DFT exploration of the various binding modes shown in Figure 1, along with predicted KIEs that match experimental measurements, confirms that C-C bond-formation occurs via binding mode B. The results presented here provide *the first "experimental picture" of the transition state of this seminal reaction in bifunctional thiourea catalysis.*

## Results and discussion

### A. Experimental Kinetic Isotope Effects

The prototypical reaction of **1a** and **2a** catalyzed by **3** was chosen for our mechanistic study. The KIEs for all carbon atoms of **1a** and **2a** were simultaneously determined using NMR methodology at natural abundance from starting material analysis.<sup>17</sup> Using a slightly modified version of Takemoto's procedure (**1a:2a** of 1.25:1 instead of 2:1), reactions were taken to ~80% conversion in **2a** (and ~65% in **1a**) as determined by proton NMR analysis. Unreacted **1a** and **2a** were then reisolated from the reaction mixture and the <sup>13</sup>C isotopic composition was compared to samples of **1a** and **2a**, not subjected to reaction conditions. From the fractional conversions and the isotopic enhancements, <sup>13</sup>C KIEs were calculated using standard methodology (Fig 2).<sup>18</sup>

Observation of a significant primary (~3%) <sup>13</sup>C KIE on C1 of **1a** and C1' of **2a** (Fig 2) suggests that both C1 and C1' are involved in the rate-determining transition state. The qualitative interpretation of these measurements is that carbon-carbon bond formation (**TS2**) is the first irreversible step of the catalytic cycle – an interpretation that is consistent with earlier studies

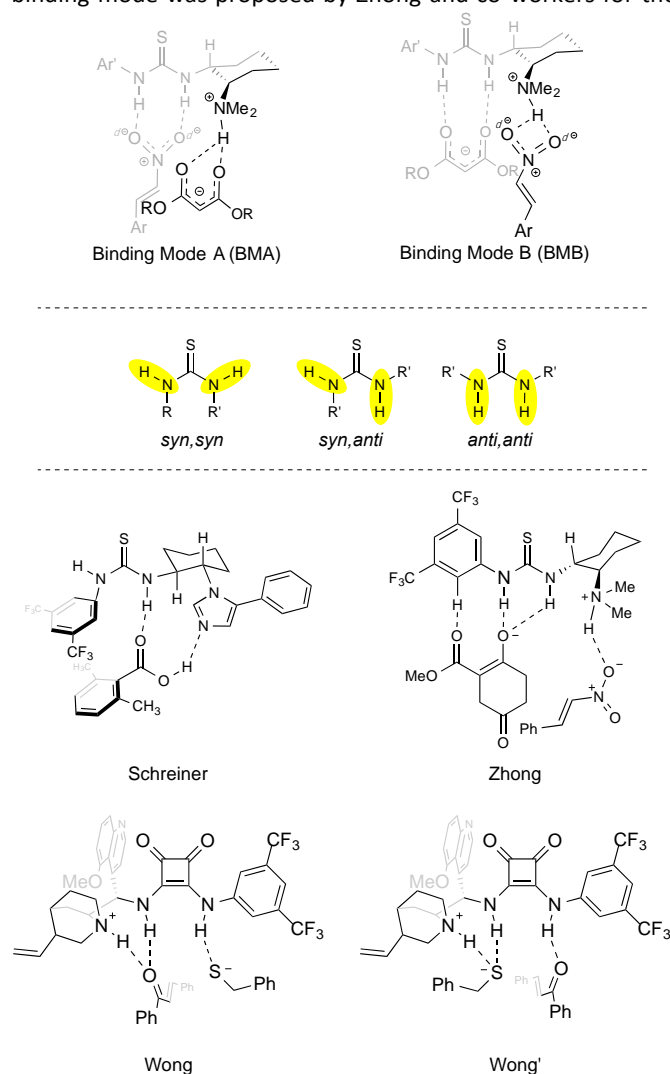


**Figure 1.** Reported binding modes for the bifunctional thiourea catalysis in various reactions reported in the literature.

by Takemoto and Pápai.<sup>10, 11b</sup> This interpretation is, however, inconsistent with rate-determining C-protonation of the nitronate (**TS3** - the Liu proposal<sup>10a</sup>) since such a step would exhibit a primary <sup>13</sup>C KIE on C2' of **2a** and negligible <sup>13</sup>C KIEs on C1 of **1a** and C1' of **2a**.

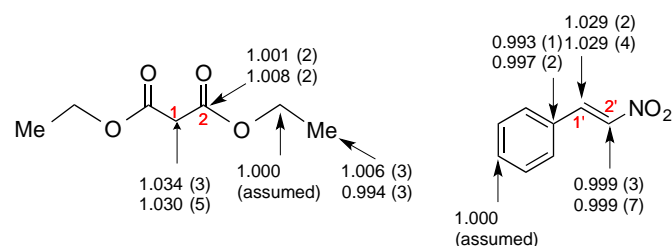


**Figure 2.** Experimentally measured KIEs for the enantioselective Michael addition of **2a** to **1a** catalyzed by **3**.

### B. Theoretical Structures

A quantitative interpretation of our experimental KIEs involved the DFT calculations of transition structures for each step in the catalytic cycle for the reaction of **1a** and **2a** catalyzed by **3**. The full system (89 atoms) was computed using the B3LYP method and a 6-31+G\*\* basis set.<sup>19</sup> A polarizable continuum model (PCM) for toluene, as implemented in Gaussian09, was employed to account for the effects of the reaction solvent.<sup>20</sup> This methodology is well supported in the literature and has been shown to accurately describe the energetics of other bifunctional thiourea-catalyzed reactions.<sup>21</sup> To evaluate the relative energetics of the transition structures leading to the two enantiomers, single point energies were obtained using B3LYP-D3(BJ)/6-311++G\*\* PCM (toluene).<sup>22</sup> The computed relative free energies ( $\Delta\Delta G^\ddagger$ ) are extrapolated Gibbs free energies obtained by adding the free energy correction from the B3LYP/6-31+G\*\* PCM (toluene) optimization to the high-level single point energy calculation. This is the first theoretical study, performed at a high level of theory, on the full system originally reported by Takemoto. Such a thorough theoretical study is expected to provide highly precise KIE predictions for comparison with experiment. A rigorous exploration for the lowest energy structure for C-C bond formation (**TS2**), the enantioselectivity determining step, was performed using DFT calculations based upon existing models in the literature (Fig 1) as well as a conformational search using quantum mechanical simulations as implemented in DFTB+ as detailed below.<sup>23</sup>

The four lowest energy structures from our thorough explorations are shown in Fig 3 along with their relative free energies ( $\Delta\Delta G^\ddagger$ ). An initial search based on the binding modes previously reported in the literature, resulted in the lowest energy transition structure akin to binding mode B – **TS2<sub>BMB-S</sub>** leading to the major enantiomer and **TS2<sub>BMB-R</sub>** for the minor enantiomer of product (Fig 3). Additionally, a comprehensive search of transition structures for **TS2** was carried out by modifying (a) the H-bonding contacts, (b) *anti* vs *syn* conformation of the thiourea, and (c) position of the substrates with regard to the bifunctional thiourea. To further ensure that we had explored the large conformational space involved in the system, a thorough search was conducted using the quantum mechanical method DFTB+ with the Slater-Koster parameters.<sup>24</sup>

Simulations were initiated from several of the lowest energy binding modes for both the major and minor enantiomers.<sup>25</sup> Starting from the geometry of the lowest energy structures derived from these conformational dynamics, transition structures were located in Gaussian using B3LYP/6-31+G\*\* PCM (toluene). Despite these extensive explorations of the reaction space, **TS2<sub>BMB-S</sub>** was still found to be the lowest energy transition structure leading to the major enantiomer. The lowest energy transition structure leading to the minor enantiomer (**TS2<sub>BMB-R</sub>**) was 2.4 kcal/mol higher in energy than **TS2<sub>BMB-S</sub>**. This corresponds to a predicted ee of 97% (*S*), a result that is consistent with the 93% ee (*S*) observed for this reaction. Our extensive explorations led to the identification of an additional minor enantiomer transition structure **TS2<sub>Wong-R</sub>**, corresponding to the binding mode proposed by Wong and co-workers. This transition structure was calculated to be 3.3 kcal/mol higher in energy than **TS2<sub>BMB-S</sub>** (0.9 kcal/mol higher in energy than **TS2<sub>BMB-R</sub>**). Finally, the second lowest energy transition structure leading to the major enantiomer was **TS2<sub>BMA-S</sub>**, which was found to be 4.7 kcal/mol higher in energy than **TS2<sub>BMB-S</sub>**. This result provides strong support that the reaction likely proceeds via binding mode B. Structures found using alternative binding modes and those located from dynamic simulations that are higher in energy than the structures in Figure 3 are included in the Supporting Information.

The origin of catalysis for the bifunctional thiourea catalyzed Michael addition can be understood by examining the interactions between the catalyst-substrate complex. At the transition state for C-C bond formation, the greatest build-up of negative charge is on the oxygen atoms of the nitro group of **2a**. Interactions from the catalyst that stabilize this electron sink should have the greatest effect in lowering the energy of the transition state. Catalyst **3** possesses H-bonding sites at the two thioamide thiourea moieties as well as the protonated tertiary amine – the strongest H-bonding donor. Structures which optimize these interactions are the most favored; additional stability can arise from non-conventional H-bonding interactions between the acidic aromatic hydrogens next to the CF<sub>3</sub> groups of the catalyst, as well as CHO interactions from the methyl groups of the protonated tertiary amine. Transition structure **TS2<sub>BMB-S</sub>** is stabilized by an H-bond (1.70 Å) between the protonated tertiary amine and the negatively charged oxygen of the nitro group of **2a**. The nucleophilic malonate is stabilized by H-bonds from the thioamide hydrogens of **3** to the oxygen atoms of **1a** (1.89 Å, 1.87 Å). In addition, one Ar-H bond (2.52 Å) contributes to malonate stabilization. Similar interactions are found in the Binding Mode B minor isomer **TS2<sub>BMB-R</sub>**, the nitro group of **2a** is stabilized solely by an H-bond to the protonated amine (1.72 Å), and the malonates are stabilized by H-bonds to the amides of the thiourea (1.82 Å, 1.87 Å). In **TS2<sub>BMA-S</sub>** the H-bonding partners are flipped, the protonated amine of the catalyst stabilizes the malonate and the thioamide hydrogens stabilize the nitro moiety. The higher energy of transition structures in binding mode A indicates that this is a less energetically stable configuration for catalysis. Finally, in **TS2<sub>Wong-R</sub>** the nitro group is stabilized by two H-bonds (one thioamide 1.88 Å, one protonated amine 1.83 Å) and the

malonate is stabilized by one amide H-bond (1.92 Å) and one CHO interaction (2.23 Å) with the slightly acidic methyl hydrogen of the protonated tertiary amine moiety.

The origin of enantioselectivity for this reaction can be understood using the above interaction analysis. The transition structure  $TS2_{BMB-S}$  and  $TS2_{BMB-R}$ , possess very similar H-bonding networks, though they differ by 2.4 kcal/mol. The difference in energy between *R* and *S* can best be explained by examining the geometry around the forming C-C bond. In order to accommodate the stabilizing interactions with the catalyst, the forming C-C bond in  $TS2_{BMB-S}$  adopts a staggered conformation of the substituents (dihedral angle of  $\sim 60^\circ$  between the alkene of **2a** and the ester groups of **1a**); conversely, transition structure  $TS2_{BMB-R}$  has a more eclipsed configuration for these groups (dihedral  $\sim 30^\circ$ ) as the C-C bond forms. The resulting increased steric interactions between substrates in  $TS2_{BMB-R}$

compared to  $TS2_{BMB-S}$  is the most likely origin of enantioselectivity in this reaction.

We also located transition structures for the first and third steps of the catalytic cycle ( $TS1$  and  $TS3$ , Scheme 2), deprotonation of **1a** by **3** and protonation of product nitronate by  $3H^+$  respectively. Transition structure  $TS1_{C-dep}$  for the deprotonation of the keto-form of **1a** by the amine moiety of **3** is lower in energy by 1.5 kcal/mol ( $\Delta\Delta G^\ddagger$ ) than  $TS1_{O-dep}$ , the transition state for deprotonation of the enol form of **1a**. As for  $TS3$ , transition structure  $TS3_{C-prot}$  for the protonation at the nitronate carbon by the protonated amine moiety of **3** is higher in energy by 17.9 kcal/mol ( $\Delta\Delta G^\ddagger$ ) than  $TS3_{O-prot}$ , the transition structure for protonation at the nitronate oxygen. This suggests that the final protonation takes place at the nitronate oxygen.<sup>25</sup> Our experimental isotope effects indicate the ensuing

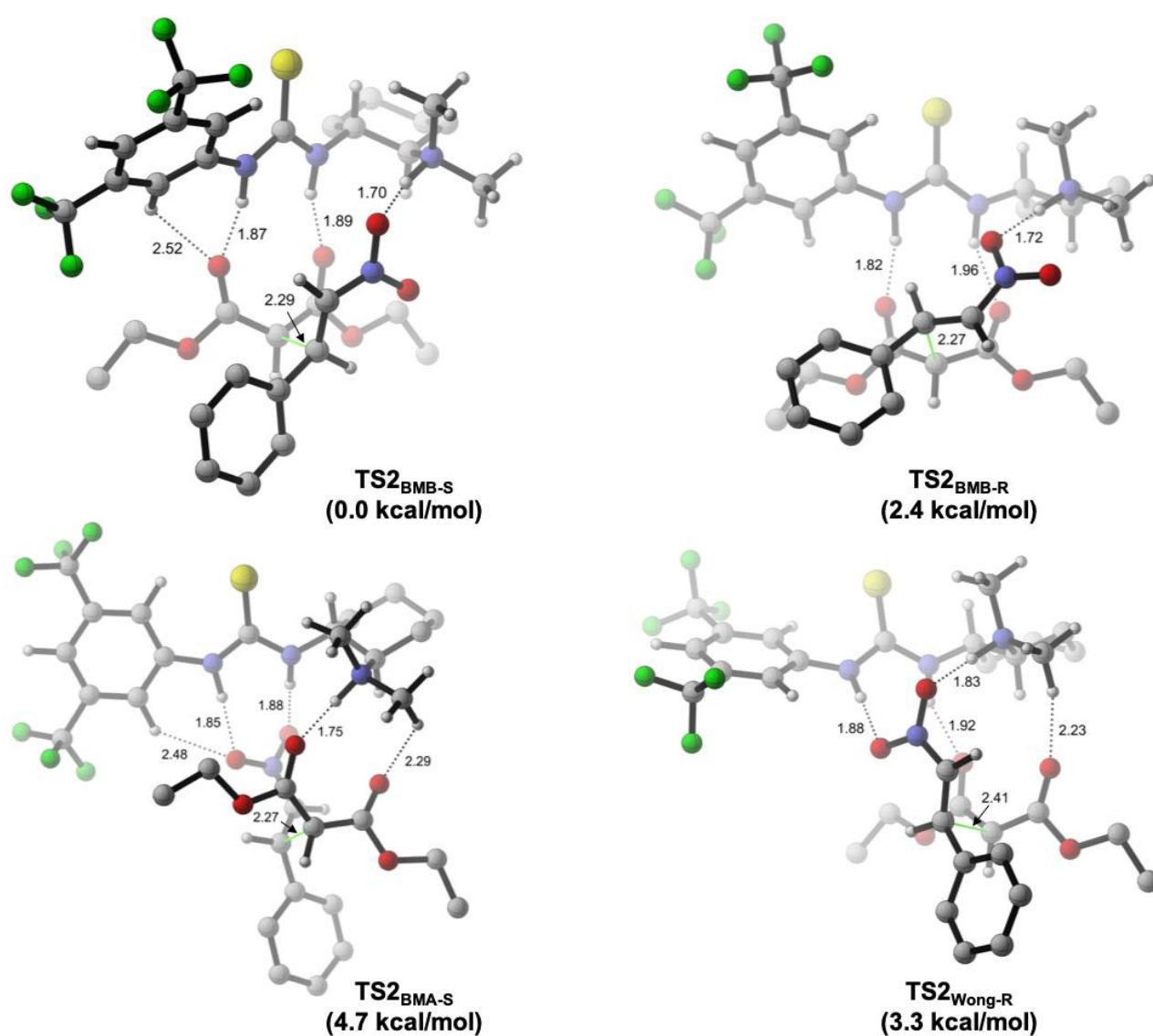
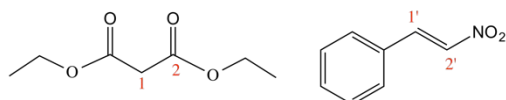


**Figure 3.** Four lowest energy transition structures for the Michael reaction of **1a** with **2** catalyzed by **3**.  $TS2_{BMB-S}$  is favoured by 3.1 kcal/mol, consistent with experiment. Important H-bonding interactions are indicated with dotted lines and shown in Angstroms. The relative free energies ( $\Delta\Delta G^\ddagger$ ) are shown in parentheses.

tautomerization leading to the final C-protonated product is a facile process, since no KIE is observed on C2'.<sup>26</sup>

### C Calculated KIEs

As a final step, quantitative interpretation of our experimental KIEs, predicted <sup>13</sup>C KIEs were obtained from the scaled vibrational frequencies of the respective transition structures using the program ISOEFF98.<sup>27</sup> A Wigner tunneling correction was applied to all predicted KIEs.<sup>28</sup> The resulting <sup>13</sup>C KIE predictions at the key carbon atoms of **1a** and **2a** for **TS1**, **TS2**, and **TS3** along with a comparison to corresponding experimental values are presented in Table 1.



Transition State	1-C	2-C	1'-C	2'-C
TS1 <sub>C-dep</sub>	1.011	1.005	N/A	N/A
TS1 <sub>O-dep</sub>	1.001	1.010	N/A	N/A
TS2 <sub>BMB-S</sub>	1.032	1.007	1.031	0.999
TS3 <sub>C-dep</sub>	0.994	0.999	1.000	1.015
TS3 <sub>O-dep</sub>	0.996	1.000	1.000	0.993
Experimental KIEs	1.030 (5)	1.008 (2)	1.029 (4)	0.999 (7)
	1.034 (3)	1.001 (2)	1.029 (2)	0.999 (3)

**Table 1.** Predicted <sup>13</sup>C KIEs for the key carbon atoms of **1a** and **2a** for all computed transition structures and comparison to corresponding experimental KIEs.

The interpretation of the comparison of experimental and theoretical KIEs is unambiguous. The predicted KIEs for lowest energy carbon-carbon bond-forming transition state (**TS2<sub>BMB-S</sub>**) are in excellent agreement with the experimental KIEs for the bond-forming carbon atoms of both **1a** (1.032 on C1) and **2a** (1.031 on C1'). This provides strong evidence for a mechanism involving rate-determining carbon-carbon bond formation – a

result consistent with prior experimental studies by Takemoto and computational studies by Pápai.<sup>10, 11</sup> DOI: 10.1039/C9OB00072K

### Conclusions

The combination of experimental <sup>13</sup>C KIEs and theoretical calculations presented herein provide strong evidence for rate-determining C-C bond formation in the bifunctional thiourea catalyzed enantioselective addition of diethylmalonate to *trans*-β-nitrostyrene. Our results provide the first “experimental” picture of the key enantioselectivity-determining transition state of this seminal reaction in bifunctional thiourea organocatalysis.

### Conflicts of interest

There are no conflicts to declare.

### Acknowledgement

Financial support for this work was provided by Binghamton University startup funds and NIGMS (R01 GM126283). M.J.V. J.S.H and J.A.I. acknowledge support from the National Science Foundation through XSEDE resources provided by the XSEDE Science Gateways Program.

### Notes and references

Experimental procedures, theoretical methodology, and coordinates of all calculated structures and product characterization data. This material is included in the Supporting Information.

<sup>1</sup> T. Okino, Y. Hoashi, Y. Takemoto, *J. Am. Chem. Soc.*, 2003, **125**, 12672–12673.

<sup>2</sup> T. Okino, S. Nakamura, T. Furukawa, Y. Takemoto, *Org. Lett.* 2004, **6**, 625–627.

<sup>3</sup> A. Berkessel, F. Cleemann, S. Mukherjee, T. N. Müller, J. Lex, *Angew. Chemie - Int. Ed.* 2005, **44**, 807–811.

<sup>4</sup> Y. Hoashi, T. Okino, Y. Takemoto, *Angew. Chemie - Int. Ed.* 2005, **44**, 4032–4035.

<sup>5</sup> S. Sakamoto, N. Kazumi, Y. Kobayashi, C. Tsukano, Y. Takemoto, *Org. Lett.* 2014, **16**, 4758–4761.

<sup>6</sup> M. S. Manna, S. Mukherjee, *J. Am. Chem. Soc.* 2015, **137**, 130–133.

<sup>7</sup> N. Yoneda, Y. Fukata, K. Asano, S. Matsubara, *Angew. Chemie - Int. Ed.* 2015, **54**, 15497–15500.

<sup>8</sup> Selected examples include (a) Y. Takemoto, *Org. Biomol. Chem.* 2005, **3**, 4299–4306. (b) Y. Takemoto, *Chem. Pharm. Bull.* 2010, **58**, 593–601. (c) W. Y. Siau, J. Wang, *Catal. Sci. Technol.* 2011, **1**, 1298–

1310. (d) T. J. Auvil, A. G. Schafer, A. E. Mattson, *European J. Org. Chem.* 2014, 2633–2646.

<sup>9</sup> *Science of Synthesis: Asymmetric Organocatalysis II*; List, B., Maruoka, K., Eds.; Thieme: Stuttgart, Germany, 2012. pp 437. I'm not sure how this Journal wants books cited.

<sup>10</sup> T. Okino, Y. Hoashi, T. Furukawa, X. Xu, Y. Takemoto, *J. Am. Chem. Soc.* 2005, **127**, 119–125.

<sup>11</sup> (a) R. Zhu, D. Zhang, J. Wu, C. Liu, *Tetrahedron Asymmetry* 2006, **17**, 1611–1616.; (b) A. Hamza, G. Schubert, T. Soós, I. Pápai *J. Am. Chem. Soc.* 2006, **128**, 13151–13160.

<sup>12</sup> A selection of computational papers that have investigated the binding modes on this and similar systems are listed here (a) T. Azuma, Y. Kobayashi, K. Sakata, T. Sasamori, N. Tokitoh, Y. Takemoto, *J. Org. Chem.* 2014, **79**, 1805–1817. (b) A. Sengupta, R. B. Sunoj, *J. Org. Chem.* 2012, **77**, 10525–10536. (c) T. E. Shubina, M. Freund, S. Schenker, T. Clark, S. B. Tsogoeva, *Beilstein J. Org. Chem.* 2012, **8**, 1485–1498. (d) C. Trujillo, I. Rozas, A. Botte, S. J. Connon, *Chem. Commun.* 2017, **53**, 8874–8877. (e) A. Quintard, D. Cheshmedzhieva, M. d. M. Sanchez Duque, A. Gaudel-Siri, J. V.

- Naubron, Y. Génisson, J. C. Plaquevent, X. Bugaut, J. Rodriguez, T. Constantieux, *Chem. - A Eur. J.* 2015, **21**, 778–790. (f) X. Li, Y. Y. Zhang, X. S. Xue, J. L. Jin, B. X. Tan, C. Liu, N. Dong, J. P. Cheng, *European J. Org. Chem.* 2012, **2**, 1774–1782. (g) M. N. Grayson, *J. Org. Chem.* 2017, **82**, 4396–4401. (h) M. N. Grayson, K. N. Houk, *J. Am. Chem. Soc.* **2016**, *138*, 9041–9044.
- <sup>13</sup> B. Tan, Y. Lu, X. Zeng, P. J. Chua, G. Zhong, *Org. Lett.* 2010, **12**, 2682–2685.
- <sup>14</sup> F. Esteban, W. Ciešlik, E. M. Arpa, A. Guerrero-Corella, S. Díaz-Tendero, J. Perles, J. A. Fernández-Salas, A. Fraile, J. Alemán, *ACS Catal.* 2018, **8**, 1884–1890.
- <sup>15</sup> J. Guo, M. W. Wong, *J. Org. Chem.* 2017, **82**, 4362–4368.
- <sup>16</sup> (a) Z. Zhang, K. M. Lippert, H. Hausmann, M. Kotke, P. R. Schreiner, *J. Org. Chem.* 2011, **76**, 9764–9776. (b) A. Supady, S. Hecht, C. Baldauf, *Org. Lett.* 2017, **19**, 4199–4202. (c) N. Hayama, R. Kuramoto, T. Földes, K. Nishibayashi, Y. Kobayashi, I. Pápai, Y. Takemoto, *J. Am. Chem. Soc.* 2018, **140**, 12216–12225. (d) M. Heshmat, *J. Phys. Chem. A* 2018, **122**, 7974–7982. (e) Á. Madarász, Z. Dósa, S. Varga, T. Soós, A. Csámpai, I. Pápai, *ACS Catal.* 2016, **6**, 4379–4387. (f) G. Tárkányi, P. Király, T. Soós, S. Varga, *Chem. - A Eur. J.* 2012, **18**, 1918–1922.
- <sup>17</sup> D. A. Singleton, A. A. Thomas, *J. Am. Chem. Soc.* 1995, **117**, 9357–9358.
- <sup>18</sup> See supporting information for details.
- <sup>19</sup> (a) A. D. Becke, *J. Chem. Phys.* 1993, **98**, 5648–5652. (b) C. Lee, W. Yang, R. G. Parr, *Phys. Rev. B* 1998, **37**, 785–789. (c) P. J. Stephens, F. J. Devlin, C. F. Chabalowski, M. J. Frisch, *J. Phys. Chem.* 1994, **98**, 11623–11627.; (d) P. C. Hariharan, J. A. Pople, *Theor. Chim. Acta* 1973, **213**, 213–222.
- <sup>20</sup> (a) C. Amovilli, V. Barone, R. Cammi, E. Cancès, M. Cossi, B. Mennucci, C. S. Pomelli, J. Tomasi, *J. Adv. Quantum Chem.* 1998, **32**, 227–261. (b) See supporting information for full *Gaussian09* citation
- <sup>21</sup> (a) S. J. Zuend, E. N. Jacobsen, *J. Am. Chem. Soc.* 2007, **129**, 15872–15883. (b) S. J. Zuend, E. N. Jacobsen, *J. Am. Chem. Soc.* 2009, **131**, 15358–15374. (c) H. Xu, S. J. Zuend, M. G. Woll, Y. Tao, E. N. Jacobsen, *Science* 2010, **327**, 986–990.
- <sup>22</sup> (a) S. Grimme, S. Ehrlich, L. Goerigk, *J. Comput. Chem.* 2011, **32**, 1456–1465. (b) R. Krishnan, J. S. Binkley, R. Seeger, J. A. Pople, *J. Chem. Phys.* 1980, **72**, 650–654.
- <sup>23</sup> B. Aradi, B. Hourahine, T. Frauenheim, *J. Phys. Chem. A* 2007, **111**, 5678–5684.
- <sup>24</sup> (a) M. Elstner, D. Porezag, G. Jungnickel, J. Elsner, M. Haugk, T. Frauenheim, S. Suhai, G. Seifert, *Phys. Rev. B* 1998, **58**, 7260–7268. (b) J. C. Slater, G. F. Koster, *Phys. Rev.* 1954, **94**, 1498–1524. (c) D. A. Papaconstantopoulos, *Handbook of the Band Structure of Elemental Solids*; Plenum Press: New York, 1986.
- <sup>25</sup> Computational details and cartesian coordinates for TS1 and TS3 are included in the Supporting Information.
- <sup>26</sup> We were unable to locate a tautomerization transition structure for **TS3<sub>O-prot</sub>** that was lower in energy than C-C bond formation. **TS3<sub>O-prot</sub>** may be reversible and final protonation occurs at the carbon (**TS3<sub>C-prot</sub>**), though the energy for this transition structure is also higher than C-C bond formation. However, the most likely scenario is that DFT fails to correctly predict the energies of proton transfers with respect to C-C bond formation. See Plata, R. E.; Singleton, D. A. *J. Am. Chem. Soc.* **2015**, *137*, 3811–3826. A detailed discussion on the energetics of the given Michael reaction as well as the limitations of DFT calculations in predicting relative energies of transition structures with and without proton transfers is included in the Supporting Information (S17).
- <sup>27</sup> V. Anisimov, P. Paneth, *J. Math. Chem.* 1999, **26**, 75–86.
- <sup>28</sup> E. P. Wigner, *Phys. Chem.* 1932, **B19**, 203.

